Article

Evaluation of the Carbene Hydride Mechanism in the Carbon#Carbon Bond Formation Process of Alkane Metathesis through a DFT Study

Sandra Schinzel, Henry Chermette, Christophe Cope#ret, and Jean-Marie Basset

J. Am. Chem. Soc., **2008**, 130 (25), 7984-7987 • DOI: 10.1021/ja800474h • Publication Date (Web): 30 May 2008

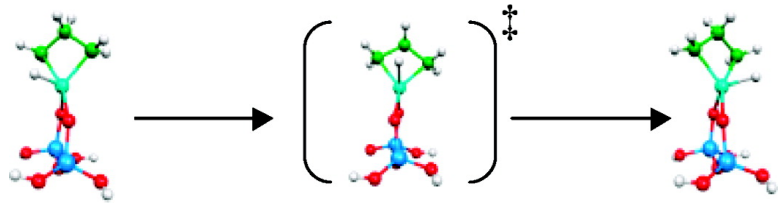

J|A|C|S
ARTICLES

Published on Web 05/30/2008

Evaluation of the Carbene Hydride Mechanism in the Carbon−Carbon Bond Formation Process of Alkane Metathesis through a DFT Study

Sandra Schinzel,[†] Henry Chermette,*[,†] Christophe Copéret,[‡] and Jean-Marie Basset[‡]

Université Lyon-1, Laboratoire de Chimie-Physique Théorique, Université de Lyon, and CNRS UMR 5180 Sciences Analytiques, Bât Dirac, 43 Bd du 11 Novembre 1918, 69622 Villeurbanne Cedex, France, Université de Lyon, Institut de Chimie de Lyon, C2P2-CNRS-Equipe LCOMS ESCPE Lyon, F-308-43 Boulevard du 11 Novembre 1918 F-69616 Villeurbanne Cedex, France

Received January 21, 2008; E-mail: henry.chermette@univ-lyon1.fr

Abstract: Olefin metathesis on a silica supported tantalumhydridocarbene complex, the key carbon−carbon making process in alkane metathesis, requires a large number of elementary steps in contrast to the known olefin metathesis pathway, which corresponds to successive [2 + 2]-cycloaddition and cycloreversion steps. The direct pathway is forbidden because it requires the formation of a high energy reaction intermediates, an olefin adduct of trigonal bipyramid (TBP) geometry, where the carbene is trans to an hydride ligand. Extra low-energy steps are therefore necessary to connect the reactants to products, the key being a turnstile interconversion at the metallacyclobutane intermediates.

Introduction

Alkane metathesis corresponds to the transformation of a given alkane into its higher and lower homologues.[1,2] Recent kinetic and structure−reactivity investigations have shown that the elementary steps of carbon−carbon bond cleavage and formation are similar to those of olefin metathesis and probably involve metallocarbene hydride intermediates (Scheme 1).[3−5] Mikhailov et al. have reported an alkane metathesis mechanism based on similar propagating carbenic species, but with different C−C bond formation and cleavage steps based on alkyl migration and α-alkyl transfer elementary steps.[6] However, this mechanism is not consistent with the kinetic studies and the observed product distribution in alkane metathesis.[4] We have therefore investigated the reaction of ethene with the proposed alkylidene hydrido tantalum intermediate through DFT calculations.

Modeling studies have been achieved using $[(\equiv SiO)_2Ta(=CH_2)H]$ (**1s**) as the active site (Scheme 2).[4] All the calculations were performed using a silica model made of a small cluster of two silicon atoms (**1**), in which the dangling bonds are modeled by OH groups (Scheme 2). Simple small SiO_2 clusters with the minimum number of Si atoms are typically sufficient to represent the active site of silica supported materials.[7,8] We have limited our theoretical investigation to the carbon−carbon bond formation and cleavage processes, and more specifically, we have investigated the reaction of $[(Si_mO)_2Ta(=CH_2)H]$ (**1**) with a representative olefin, ethene.

Computational Details

These calculations were performed with the ADF2006 code,[9,10] using a double ζ basis set augmented by a polarization function (DZP) for the whole reaction path (Figure 1 and Tables S1 and S2 of the Supporting Information). Geometry optimizations were carried out without any symmetry restriction. The nature of the extrema (minimum and transition state structures) was verified with frequency calculations (caption of Figure 1b). The intrinsic reaction coordinate (IRC) has been followed to confirm that transition states connect to reactants and products.[11] Small frozen cores approximation has been used for shells up to 1s for O, 2p for Si, and 4d for Ta. Relativistic effects were taken into account through the frozen core density (Dirac code to build them

[†] Laboratoire de Chimie-Physique Théorique.
[‡] C2P2-CNRS-Equipe LCOMS.

(1) Vidal, V.; Theolier, A.; Thivolle-Cazat, J.; Basset, J.-M. *Science* **1997**, *276*, 99–102.
(2) (a) Maury, O.; Lefort, L.; Vidal, V.; Thivolle-Cazat, J.; Basset, J.-M. *Angew. Chem., Int. Ed.* **1999**, *38*, 1952–1955. (b) Basset, J.-M.; Copéret, C.; Soulivong, D.; Taoufik, M.; Thivolle-Cazat, J. *Angew. Chem., Int. Ed.* **2006**, *45*, 6082−6085.
(3) Le Roux, E.; Chabanas, M.; Baudouin, A.; de Mallmann, A.; Copéret, C.; Quadrelli, E. A.; Thivolle-Cazat, J.; Basset, J.-M.; Lukens, W.; Lesage, A.; Emsley, L.; Sunley, G. J. *J. Am. Chem. Soc.* **2004**, *126*, 13391–13399.
(4) Basset, J. M.; Copéret, C.; Lefort, L.; Maunders, B. M.; Maury, O.; Le Roux, E.; Saggio, G.; Soignier, S.; Soulivong, D.; Sunley, G. J.; Taoufik, M.; Thivolle-Cazat, J. *J. Am. Chem. Soc.* **2005**, *127*, 8604–8605.
(5) Le Roux, E.; Taoufik, M.; Copéret, C.; de Mallmann, A.; Thivolle-Cazat, J.; Basset, J.-M.; Maunders, B. M.; Sunley, G. J. *Angew. Chem., Int. Ed.* **2005**, *44*, 6755–6758.
(6) Mikhailov, M. N.; Kustov, L. M. *Russ. Chem. Bull.* **2005**, *54*, 300–311.
(7) Mikhailov, M. N.; Bagatur yants, A. A.; Kustov, L. M. *Russ. Chem. Bull.* **2003**, *52*, 30–35.
(8) (a) Copéret, C.; Grouiller, A.; Basset, M.; Chermette, H. *ChemPhysChem* **2003**, *4*, 608–611. (b) Solans-Monfort, X.; Filhol, J.-S.; Copéret, C.; Eisenstein, O. *New J. Chem.* **2006**, *30*, 842−850.
(9) Te Velde, G.; Bickelhaupt, F. M.; Baerends, E. J.; Fonseca Guerra, C.; Van Gisbergen, S. J. A.; Snijders, J. G.; Ziegler, T. *J. Comput. Chem.* **2001**, *22*, 931–967.
(10) Baerends, E. J. et al. ADF 2006.01, SCM, Theoretical Chemistry, Vrije Universiteit, Amsterdam, The Netherlands.
(11) Deng, L.; Ziegler, T.; Fan, L. *J. Chem. Phys.* **1993**, *99*, 3823–3835.

10.1021/ja800474h CCC: $40.75

Scheme 1

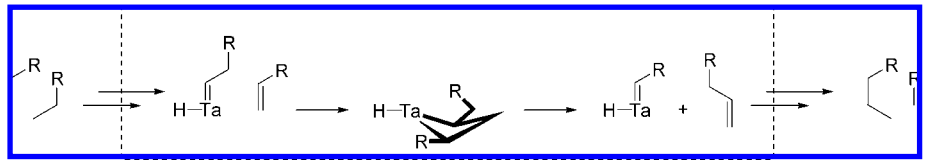

Scheme 2

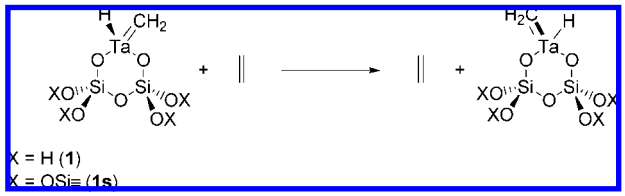

Scheme 3

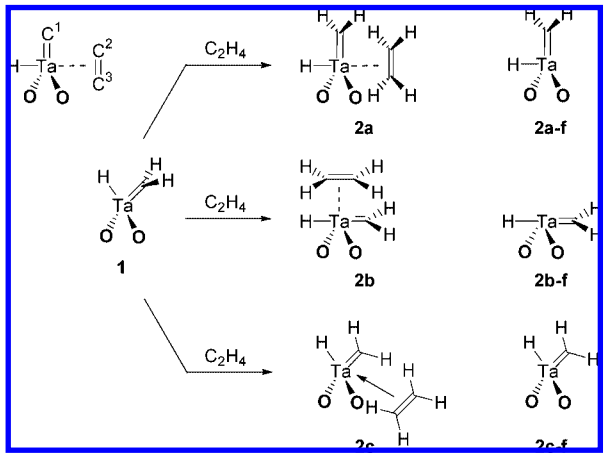

Scheme 4

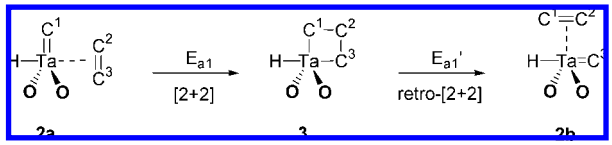

within ADF) and the ZORA approach.[10,12] The adapted basis set ZORA/DZP of ADF and the PW91 gradient-corrected (GGA) exchange-correlation functional have been used.[13]

Results and Discussions

The potential energy surface of the reaction pathway, which connects reactants to products, shows that the reaction of [(Si$_m$O)$_2$Ta(=CH$_2$)H] and ethene is more complex than expected (Figure 1a). Previous theoretical studies on olefin metathesis have already shown that instead of a classical two-step process (Chauvin mechanism),[14–18] olefin metathesis involves extra steps because of the formation of an olefin adduct, a step required even for d^0 systems.[19,20] Here, the reaction is yet even more complex, because [2 + 2]-cycloaddition and cycloreversion are not connected via the same metallacyclobutane. The reaction pathway can be decomposed in the following blocks of events, (1) formation of an olefin adduct complex, (2) [2 + 2]-cycloaddition, and (3) interconversions of metallacyclobutanes via a turnstile process, and the following symmetrical reverse steps, metallacyclobutane interconversions, [2 + 2]-cycloreversion, and formation of the olefin and the hydrido alkylidene tantalum complex. A detailed analysis of the reaction pathway is necessary to understand the specificities of this system.

Formation of the Olefin Adduct Complex (Scheme 3). The first step corresponds to the formation of an olefin adduct. Of the possible olefin adducts **2a-c**, depending on how ethene approaches the carbene, only the lower energy olefin adduct **2a** could be obtained as a stable intermediate, which is more stable than separated reactants (**1** + ethene) by 2.5 kJ mol^{-1}. Including entropic effects shows that it is actually not a stable intermediate. The olefin adducts **2b** and **2c** could not be located, and in fact, distortion or rotation of the alkylidene ligand in **1**, giving the corresponding metal fragment without the olefin, **2b-f** and **2c-f**, cost 316.3 and 83.6 kJ mol^{-1}, while the distortion leading to **2a-f** is only slightly endoenergetic, 5.9 kJ mol^{-1}. Therefore, adducts **2b** and **2c** are probably not involved in the reaction pathway. The adduct **2a** has a distorted trigonal bipyramidal (TBP) geometry, where the carbon C^3 of the olefin occupies the apical position trans to the H ligand (Ta−C^3 = 2.516 Å, Ta−C^2 = 2.637 Å, H−Ta−C^3 = 156.4°). While the transition state **TS$_{1\to2}$** has been located and fully characterized, its energy lies below the entry point by 7 kJ mol^{-1} (Figure 1). This is probably due to two factors: the optimization of the transition state does not include entropic factors and also the presence of small interactions of ethene with the pending OH group of the model, which further stabilizes the systems with respect to separated reactants.[21]

[2 + 2]-Cycloaddition, Formation of the First Metallacyclobutane, and Direct Cycloreversion (Scheme 4). The next step is a [2 + 2]-cycloaddition, which yields, through **TS$_{2\to3}$** ($E_{a2\to3}$ = 6.5 kJ mol^{-1}), a metallacyclobutane **3** having a distorted TBP geometry (H−Ta−C^3 = 148.9 °) and being more stable than the adduct **2a** by 25.0 kJ mol^{-1}(Scheme 4). Yet, including entropic factors (Table S1), this metallacyclobutane is still less stable than separated reactants by 14.5 kJ mol^{-1} (**1** + C$_2$H$_4$). Note that the geometries of **2a** and **3** are very similar (the hydride, C^1, C^3, and Ta being in the same plane) except that the hydride in **3** is more bent toward the surface and the Ta−C^2/Ta−C^3 bonds are shorter (Tables S1 and S2 of the Supporting Information). Noteworthy, the direct [2 + 2]-cycloreversion pathway leading to

(12) Te Velde, G.; Baerends, E. J. *J. Comput. Phys.* **1992**, *99*, 84–98.
(13) Perdew, J. P. *Electronic Structure of Solids*; Academic Verlag: Berlin, 1991.
(14) Herisson, J. L.; Chauvin, Y. *Makromol. Chem.* **1971**, *141*, 161–176.
(15) Rappe, A. K.; Goddard, W. A., III *J. Am. Chem. Soc.* **1982**, *104*, 448–456.
(16) Wu, Y.-D.; Peng, Z.-H. *Inorg. Chem. Acta* **2003**, *345*, 241–254.
(17) Handzlik, J. *J. Catal.* **2003**, *220*, 23–34.
(18) Goumans, T. P. M.; Ehlers, A. W.; Lammertsma, K. *Organometallics* **2005**, *24*, 3200–3206.
(19) Solans-Monfort, X.; Clot, E.; Copéret, C.; Eisenstein, O. *J. Am. Chem. Soc.* **2005**, *127*, 14015–14025.
(20) Poater, A.; Solans-Monfort, X.; Clot, E.; Copéret, C.; Eisenstein, O. *J. Am. Chem. Soc.* **2007**, *129*, 8207–8216.
(21) The presence of the OH group in the model allows extra van der Waals interactions, leading to a stable [**1** + ethene] adduct **A**, which lies 15.9 kJ mol^{-1} lower than separated reactants; see the calculated structure in the Supporting Information.

a)

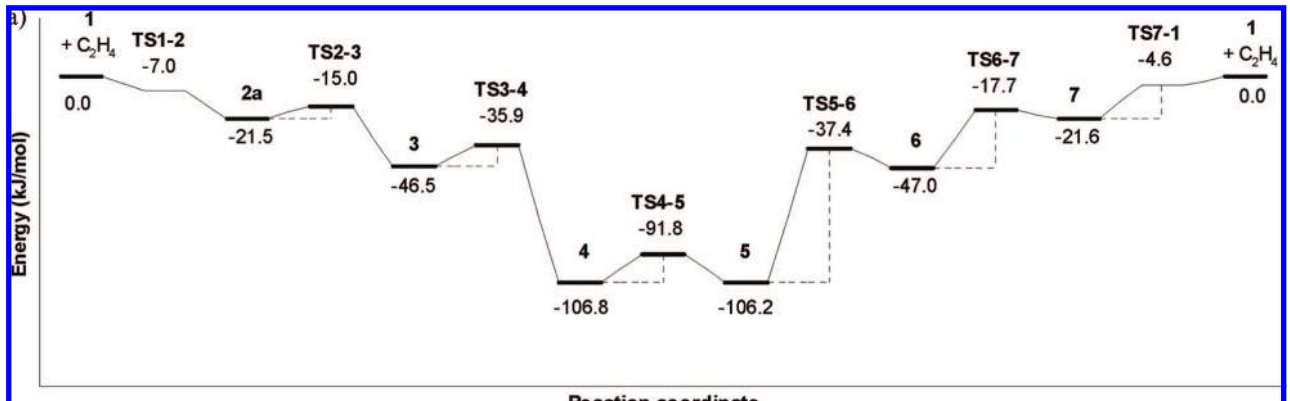

b)

Structure					
	$1+C_2H_4$	$TS_{1\rightarrow 2a}$	2a	$TS_{2a\rightarrow 3}$	3
ΔE	0	-7.0	-21.5	-15.0 (6.5)	-46.5
ΔG	0	36.7 (36.7)	27.7	42.0 (14.3)	14.5
Structure					
	$TS_{3\rightarrow 4}$	4	$TS_{4\rightarrow 5}$	5	$TS_{5\rightarrow 6}$
ΔE	-35.9 (10.9)	-106.8	-91.8 (15.0)	-106.2	-37.4 (68.2)
ΔG	22.1 (6.7)	-46.2	-34.5 (11.7)	-55.4	24.3 (77.0)
Structure					
	6	$TS_{6\rightarrow 7}$	7	$TS_{7\rightarrow 1}$	$1+C_2H_4$
ΔE	-47.0	-17.7 (21.6)	-21.6	-4.6 (17.0)	0
ΔG	9.8	43.4 (33.6)	27.3	57.1 (29.8)	0

Figure 1. (a) Potential energy surface. (b) Optimized structures, energies (electronic energy in kJ mol^{-1} after ZPE corrections with respect to **1** and ethene), and Gibbs free energies (in kJ mol^{-1} at 298 K with respect to **1** and ethene) for the main intermediates ($0-i$) and transitions states ($\mathbf{TS}_{i\rightarrow i+1}$) of the reaction pathway of the reaction of ethene and **1**. The values in parenthesis associated with the energies of $\mathbf{TS}_{i\rightarrow i+1}$represent the activation energies from *i*. All energies have been calculated using the DZP basis set (see Computational Details for more information). Imaginary frequencies of $\mathbf{TS}_{1\rightarrow 3a}$, −51.1 cm^{-1}; $\mathbf{TS}_{2a\rightarrow 3}$, −125.1 cm^{-1}; $\mathbf{TS}_{3\rightarrow 4}$; −244.0 cm^{-1}; $\mathbf{TS}_{4\rightarrow 5}$, −141.3 cm^{-1}; $\mathbf{TS}_{5\rightarrow 6}$, −109.9 cm^{-1}; $\mathbf{TS}_{6\rightarrow 7}$, −144.1 cm^{-1}; $\mathbf{TS}_{7\rightarrow 1}$, −140.1 cm^{-1}.

a putative adduct **2b** and finally to the product (**1** + C_2H_4) has not been found (Scheme 4). As already discussed, the distortion of the metal fragment from a tetrahedron in **1** into a trigonal pyramid as in **2b-f** (hydride trans to the carbene) costs 316.3 kJ mol^{-1} (Scheme 3), while this distortion costs only 5.9 kJ mol^{-1} for **2a-f** (hydride trans to an empty coordination site): this probably precludes a direct [2 + 2] cycloreversion pathway and shows that the hydride plays a key role in the mechanism.

Metallacyclobutane Interconversions and Cycloreversion (Scheme 5). The following step is thus a ligand reorganization through a low activation barrier ($E_{a3\rightarrow 4}$ = 10.7 kJ mol^{-1}) leading to a very stable metallacyclobutane (**4**): 60.3 kJ mol^{-1} more stable than **3** and much more stable than separated reactants (by 106.8 kJ mol^{-1}), even when entropic effects are included (46.2 kJ mol^{-1}). This metallacyclobutane is the most stable intermediate on the potential free energy surface, and it corresponds to a highly distorted TBP (H−Ta−C^3 = 126.6°), where the hydride, C^1, C^3, and Ta are no longer in the same plane (H−Ta−C^1−C^3 = 136.1°). With this distortion, the hydride ligand is no longer trans to an alkyl ligand (one of the MC bonds of the metallacyclobutane), a strong σ-donor ligand, hence the much greater stability of **4** vs **3**.

Scheme 5

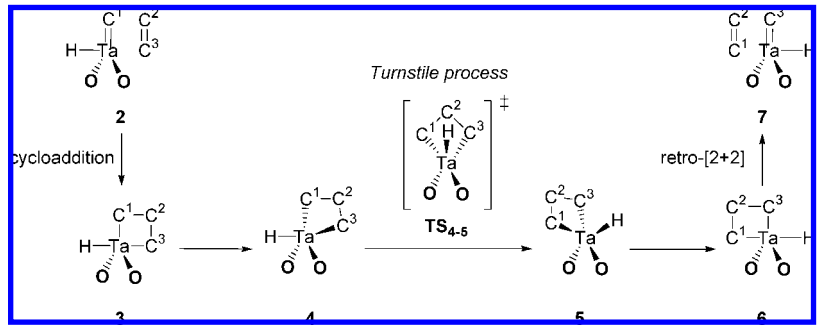

In order for the [2 + 2]-cycloreversion to take place, the metallacyclobutane **4** further reorganizes into a quasi-isoenergetic metallacyclobutanes **5** ($E_{a4\rightarrow5}$ = 14.3 kJ mol^{-1}). This step corresponds to the interconversion between two highly distorted TBP, **4** into **5**, via the transition state **TS$_{4\rightarrow5}$** having a TBP structure (H−Ta−O$_{apical}$ = 178.4°). The interconversion between **4** and **5** involves the exchange of positions of three ligands, the hydride, the carbone C^1 and the carbon C^3, the oxygen position being fixed by the bidendate bis-siloxy ligand. Of the several ways to exchange ligand positions in pentacoordinated structures (Berry pseudorotation, turnstile or other Muetterties models),[22–26] the interconversion between **4** and **5** is best described by a turnstile process (permutation of H, C^1, and C^3 vs the two oxygen atoms, Scheme 5).[26–31] Very importantly, this exchange allows the C^1 carbon to become trans to the H ligand and allows the reactants {ethene (C^{2}H$_2$═C^{3}H$_2$) and **1-C^1**) to be connected to the products (ethene (C^{1}H$_2$═C^{2}H$_2$) and **1-C^3**) through a degenerate metathesis and nearly symmetrical reverse elementary steps of those described between **1** and **4**: step **5→6**(step **4→3**), step **6→7**(step **3→2**), and step **7→1+C$_2$H$_4$**{step **2→(1+C$_2$H$_4$)**}, the small difference in energies originating from slight differences of interaction of ethene with the OH group of the model (when OH group are left frozen through the reaction pathway, larger differences of energy and ZPE were found; data not shown). In this system, the rigid bidendate bissiloxy system used to model the silica surface forces the olefin to enter trans to the hydride ligand and precludes the direct [2 + 2]-cycloreversion, but a turnstile process allows the exchange of ligand positions to avoid a highly disfavored trans effect and thereby allows the reactants to be connected to the products through a low-energy pathway. The presence of a bidendate ligand (the surface) and a strong σ-donor ligand (an hydride ligand) is the reason for this complex reaction pathway, which has not been found for similar monodendate bisalkoxy[19] or even bidendate bisalkoxy systems having weaker σ-donor ligands.[18]

Conclusion

Olefin metathesis on a silica-supported tantalumhydridocarbene complex **1**, the key carbon−carbon making process in alkane metathesis, takes place through relatively low activation barrier processes but requires a large number of elementary steps. This is therefore a viable process of carbon−carbon bond formation in alkane metathesis, as recently proposed.[3–5] In contrast to all other investigated systems,[14–20] the short direct olefin metathesis pathway through successive [2 + 2]-cycloaddition and cycloreversion steps is forbidden, because it requires the formation of high energy reaction intermediates, an olefin adduct of TBP geometry, where the carbene is trans to an hydride ligand. Therefore, the favored pathway involves extra low-energy steps, where the symmetrical reverse steps become possible through a turnstile process at the most stable metallacyclobutane intermediates. This is a key low-energy activation step, which is necessary to connect the [2 + 2]-cycloaddition and cycloreversion steps. This illustrates that ligands (bidendate bissiloxy and the hydride) can strongly influence the reaction pathway, precluding more direct and obvious pathways.

Acknowledgment. C.C. and J.M.B. are grateful to BP Chemicals, the CNRS, and the ESCPE-Lyon for financial support. We want also to thank J. Thivolle-Cazat (LCOMS), C. Slootweg (Vrije Universiteit, Amsterdam), and K. Lammertsma (Vrije Universiteit, Amsterdam) for helpful discussions. H.C. thanks the University Lyon 1. We are also indebted to CINES (project cpt2130) for computer facilities.

Supporting Information Available: Tables S1 and S2, the full list of authors of ref 10 is provided, and the Cartesian coordinates of all intermediates and transition states have also been listed. This material is available free of charge via the Internet at http://pubs.acs.org.

JA800474H

(22) Muetterties, E. L. *J. Am. Chem. Soc.* **1969**, *91*, 4115–4122.
(23) Muetterties, E. L. *J. Am. Chem. Soc.* **1969**, *91*, 1636–1643.
(24) Berry, R. S. *J. Chem. Phys.* **1960**, *32*, 933–938.
(25) Mislow, K. *Acc. Chem. Res.* **1970**, *3*, 321–331.
(26) Ugi, I.; Marquarding, D.; Klusacek, H.; Gillespie, P.; Ramirez, F. *Acc. Chem. Res.* **1971**, *4*, 288–296.
(27) Hampton, P. D.; Daitch, C. E.; Alam, T. M.; Bencze, Z.; Rosay, M. *Inorg. Chem.* **1994**, *33*, 4750–4758.
(28) Smith, J. M.; Coville, N. J. *Organometallics* **1996**, *15*, 3388–3392.
(29) Rufinska, A.; Goddard, R.; Weidenthaler, C.; Buehl, M.; Poerschke, K.-R. *Organometallics* **2006**, *25*, 2308–2330.
(30) Gonzalez-Blanco, O.; Branchadell, V. *Organometallics* **1997**, *16*, 475–481.
(31) Yang, X.; Hall, M. B. *J. Am. Chem. Soc.* **2007**, *129*, 1560–1567.